CONTAINER SHIPS MOORED AT THE PORT OF ANTWERP: MODELLING REPSONSE TO PASSING VESSELS.

T. Van Zwijnsvoorde[1], M. Vantorre[2], S. Ides[3]

ABSTRACT

Economics of scale act as driving force for the construction of Ultra Large Container Vessels (ULCV). The biggest advantage of container vessels is fast loading and unloading of containers. Large motions of the moored vessel along the quay hamper this process and even cause safety issues. This paper focusses on modelling the behaviour of moored vessels under ship passages, using a two-step approach. The forces acting on the moored vessel are modelled using RoPES (PMH), the behaviour of the moored vessel is modelled using the Ghent University in-house time domain software Vlugmoor. In a first part, four validation cases are presented, based on GPS measurements performed at the North Sea Terminal in the port of Antwerp, where the moored vessel is a Neo-Panamax container vessel. In a second part, the mooring plan of the vessel is discussed in detail. Both on the level of the individual lines, as well as for the mooring plan, efficiency parameters are defined. These parameters express the capability of a mooring plan to deal with longitudinal and transversal forces, based on line angles and line lengths.

1 INTRODUCTION

Economics of scale lead to ever increasing ship sizes. Especially in the container shipping industry, this effect is noticeable, as the container capacity keeps on incrementing. Not only does the beam of the vessels enlarge, in steps of 1 TEU bay/row, also the number of tiers (above deck) is raised. The newest generation of container vessels which are ordered, have 24 container bays, 24 container rows and 24 tiers, which leads to the nickname 'Megamax24' vessels (Port Today, 2018). These bigger vessels are more susceptible to environmental forces. In shallow and confined waters, this has an impact on the manoeuvring capability of the vessel and the behaviour of the moored vessel at the quay. In the Port of Antwerp, channel dimensions are limited and traffic density is increasing year by year. This leads to potential movement of the moored vessel along the quay due to the passing vessel. For container vessels, these motions are highly undesirable, not only because of the impact on the efficiency of loading and unloading operations (PIANC, 2012), but also because it could pose safety issues (Van Zwijnsvoorde and Vantorre, 2017).

The behaviour of the moored vessel is the result of the action of several forces. The passing vessel's pressure field induces forces on the moored vessel, together with currents, wind and wave forces. The movement of the moored ship causes the surrounding water to move, generating hydrodynamic reactions. The mooring lines and fenders create a balance in the force equilibrium, where the characteristics of the lines and their configuration has a major impact on the motions of the vessel.

The Antwerp Port Authority executed a full-scale measurement campaign at the North Sea Terminal in 2015, the terminal in the port of Antwerp which is most exposed to passing ships and which is able to welcome deep drafted container vessels in the range of Neo-Panamax up to Ultra Large Container Vessels (Ides et al., 2018). The goal of these measurements was to find out whether ship-ship interaction effects at this terminal, which was designed and built in the 1990's, do occur and if so which parameters dominate this process at this terminal. This paper uses these measurements to validate the in-house mooring simulation package Vlugmoor, which uses input from the numerical packages Seaway and RoPES. The moored vessel used for the simulations is a 13 000 TEU vessel. The passing traffic is diverse, including a tanker, container vessel and bulk carrier. In a second part of this paper, the mooring configuration is studied, both on the level of individual lines and the mooring configuration as a whole. The efficiency of said lines and configuration is evaluated by defining a set of efficiency parameters.

[1] PhD student, Ghent University, thibaut.vanzwijnsvoorde@ugent.be

[2] Professor, Ghent University, marc.vantorre@ugent.be

[3] Research Engineer, Antwerp Port Authority, stefaan.ides@portofantwerp.com

2 MEASURING CAMPAIGN

As the port of Antwerp is the second largest (container) port in Europe (Port of Antwerp, 2017), multiple container terminals are suited for berthing the largest vessels which are in service up to this point. The port's recent developments also take into account further growth of the container vessel's size. In order to guarantee the safety of these moored vessels, during (un)loading of the containers, the port authority executed measurements of ship motions at these terminals (Ides et al., 2018).

2.1 Location

The measurement campaign at hand is performed at the North Sea Terminal (Figure 2-1), which is the most downstream river terminal of the port. It is subjected to tidal water level changes and currents. Passing vessels sail close to the moored vessels, because of the limited width of the navigational channel; The edge of the navigation channel is indicated as a green dashed line in Figure 2-1. In general, there are three different trajectories: two along the approaches to the locks *Zandvlietsluis* and *Berendrechtsluis* (1a and 1b), and one for vessels approaching to or from terminals located further upstream (2). Due to the presence of certain zones with limited water depth along the Western Scheldt and the approach channels in the North Sea, tidal windows are imposed to vessels with a draft larger than 13.1 m. This means that outbound sailing vessels may attain a considerable speed when passing the North Sea Terminal. Also, vessels need to have sufficient manoeuvrability to change course and combat the current, which demands a certain minimal speed, certainly for vessels with large lateral (wind) surfaces (e.g. RoRo, container vessels). Passing speeds over ground range between 4 and 7 m/s (8 to 14 knots), with passing distances varying between 150 m and 300 m.

Figure 2-1 : Port Of Antwerp ; Location North Sea Terminal; Three examples of passing trajectories (blue) and edge of navigational channel (green dash). – image courtesy of Antwerp Port Authority

2.2 Logged data

On a daily basis, the port authority logs a lot of information regarding the shipping traffic inside the port. At several locations, the coordinates of the vessel, the passing speed and the draft, based on AIS information, are logged. For the dedicated measuring campaign (Ides et al., 2018), moored vessel motions were registered using two GPS devices, installed on port and starboard side on the bridge, in order to monitor roll, lateral and longitudinal motions. As previous studies show (Van Zwijnsvoorde and Vantorre, 2017), the longitudinal motion is always critical for a vessel moored at a quay wall, whereas the lateral motion is rather limited. The focus will thus be on the registration of the longitudinal motion. The port requested information from the ships, concerning the mooring lines used on board.

3 VALIDATION CASES

The aim of this paper is not to present a general discussion on all the data collected during the measuring campaign (Ides et al., 2018), instead there is focussed on a selection of validation cases. For these cases, details regarding moored vessel and passing vessel are presented in chapters 3 and 5.

3.1 Moored vessel

At the North Sea Terminal, container vessels up to Ultra Large Container Vessels berth. However, most measurements were carried out on Neo-Panamax size vessels: these vessels have a length overall (L_{OA}) of 366 m and a beam (B_{OA}) of 48.2 m. They can carry a maximum of around 13 000 TEU. For the present study, two moored vessels of this type have been considered, denoted in this paper as 'C1' and 'C2'. Despite having the same main dimensions, the mooring equipment is different, which is the reason why they are considered as two separate vessels (see section 5).

3.2 Passing vessel

The passing vessel fleet is diverse, as the Port of Antwerp is an important transit port for all kinds of cargo. This means that during the stay of a containership at the terminal (typically around 36 hours), various passage events are registered. The passing events which led to the largest motions along the quay are chosen. For moored vessel C1 a tanker 'T' and an ultra large container vessel 'C3' are considered. For the second moored vessel C2, two passing bulk carriers are considered, 'B1' and 'B2'. The main dimensions of all vessels are summarized in Table 3-1. T_p is the draft of the passing vessel, T_m and h are the draft of the moored vessel and the water depth respectively, at the time of the passing event.

	C1 (=C2)	C3	T	B1	B2
L_{OA} [m]	366.0	399.0	182.6	190.4	190.4
B_{OA} [m]	48.2	53.7	32.2	32.2	32.2
T_p [m]		11.0	8.9	7.0	7.6
T_m [m]		13.6	13.7	12.6	13.1
h [m]		21.1	17.6	19.7	21.0

Table 3-1 : Main dimensions moored and passing vessels case study.

3.3 Passing distance and speed

The passing distance and speed are two important parameters, which determine the forces acting on the moored vessel due to the passing ship. Since the forces, assuming potential flow, are proportional to the speed squared, it is important to get a good estimate of this passing speed. For each passing event, the velocity and position are logged at a southern and a northern measuring station, as indicated on Figure 3-1. The input for the numerical simulation is limited to a constant velocity, which is taken as the average of both registered values. This resulting speed over ground needs to be converted to a speed through the water.

As was already shown in Figure 2-1, the passing trajectory is not a straight line. As the numerical package does not allow curved trajectories, the positions measured at both stations are connected, using a straight line (Figure 3-1). In general, outbound sailing vessels pass the moored vessel at closer distances. The vessels approaching from the river upstream will have higher velocities then the ones coming from the locks, which are still accelerating when passing the North Sea Terminal. All cases thus discuss outbound sailing vessels, following the inclined trajectory coming from the river. This means the passing distance varies during the passing event.

Figure 3-1 : Northern and southern measuring section and assumed straight trajectory. – image courtesy of Antwerp Port Authority

The average passing distance (d_{pas}) and angle (α_{pas}) relative to the quay wall are given in Table 3-2 and indicated in Figure 3-2. The passing speed is given as $U_{p,g}$ [m/s] and $U_{p,w}$ [m/s], giving the velocity registered by AIS (over ground) and the velocity through the water, taking into account the tidal current. Tanker 'T' passed during turning of the tide, where the current velocity is approximately 0 m/s.

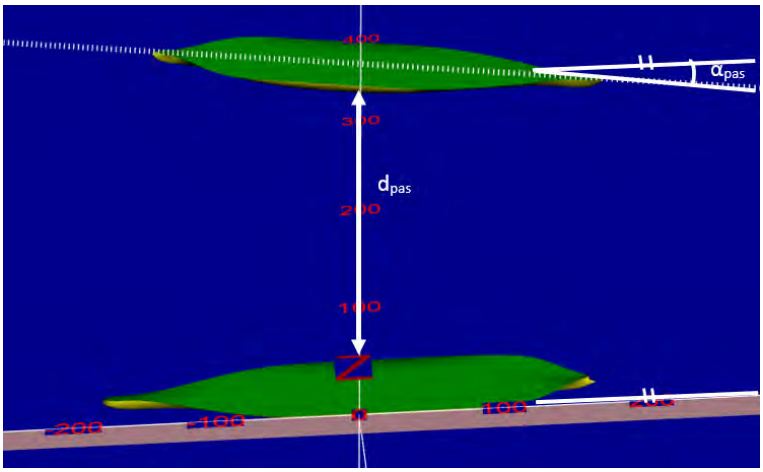

Figure 3-2 : Definition passing distance (d_{pas}) and angle (α_{pas}) for the C1-C3 case. Figure generated by RoPES.

	C3	T	B1	B2
d_{pas} [m]	292.5	205.5	241.0	205.0
α_{pas} [°]	10.3	10.1	11.4	9.6
$U_{p,g}$ [m/s]	4.9	5.6	6.4	5.8
$U_{p,w}$ [m/s]	4.1	5.6	6.0	5.1

Table 3-2 : Average passing distance (d_{pas}) and angle relative to the quay (α_{pas}); Velocity over ground ($U_{p,g}$) and through the water ($U_{p,w}$).

3.4 Time series and definition axis system

The greatest difficulty with modelling the effect of passing vessels is that it concerns a dynamic effect. The passing vessel force (surge, sway, yaw) changes in magnitude and size during the ship passage, which also leads to motions which show a time dependant variation. The relationship between exciting force and resulting motion is a function of several design parameters, as there are (added) mass of the vessel, the hydrodynamic damping and the mooring line and fender characteristics. The chosen mooring configuration and pretension level (or slack !) also influence the behaviour of the moored vessel. For

large vessels, sailing at relatively low speeds, the period of the external force and resulting motion is large. The measured longitudinal motion for the case C1-T is given in Figure 3-3. Throughout this paper, all cases are expressed by the combination of moored and passing vessel (C1-T, C1-C3, C2-B1 and C2-B2). The sign convention and axis system is shown in Figure 3-4. The moored vessel is always moored portside, with an outbound passing vessel.

The forces and motions are given in the axis system (O-x,y,z), where the x-axis is along the longitudinal symmetry plane of the vessel, the y-axis positive to portside and the z-axis positive upwards (Figure 3-4). The origin is located on the water plane, at the midship section, on the symmetry line of the vessel, in its initial position. When the passing vessel approaches the moored ship, the moored ship is attracted in positive x-direction, which means it will move ahead (indicated green in Figure 3-4) . In the second position, the ship is moved astern, according to the negative x-direction (Figure 3-4 – blue). The time (T_r) is expressed relative to the starting point of the motion, which can be seen as the starting point of the passing event. The period of the longitudinal motion (T_x), which is defined as the time between the start of the motion and the equilibrium reached after the passage, is around 160 seconds for the case C1-T. In this paper, measured data is consistently indicated with red colour, modelled results are shown using black lines.

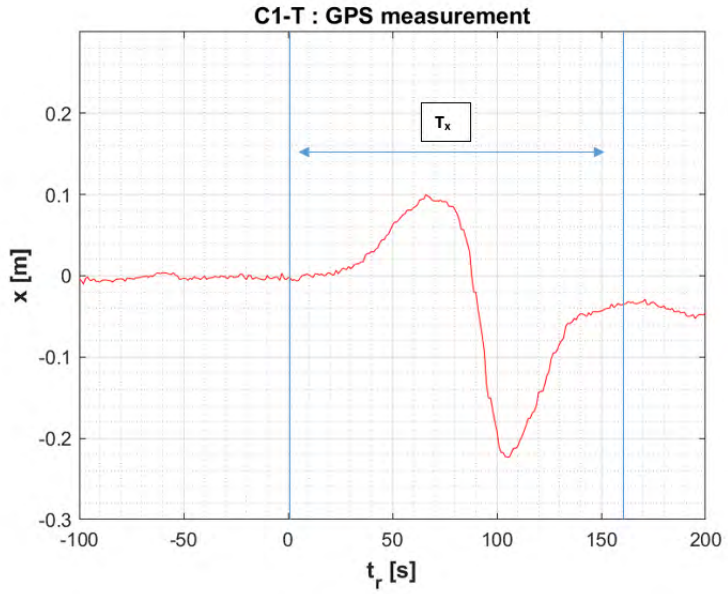

Figure 3-3 : GPS measurement of the longitudinal motion for case C1-T.

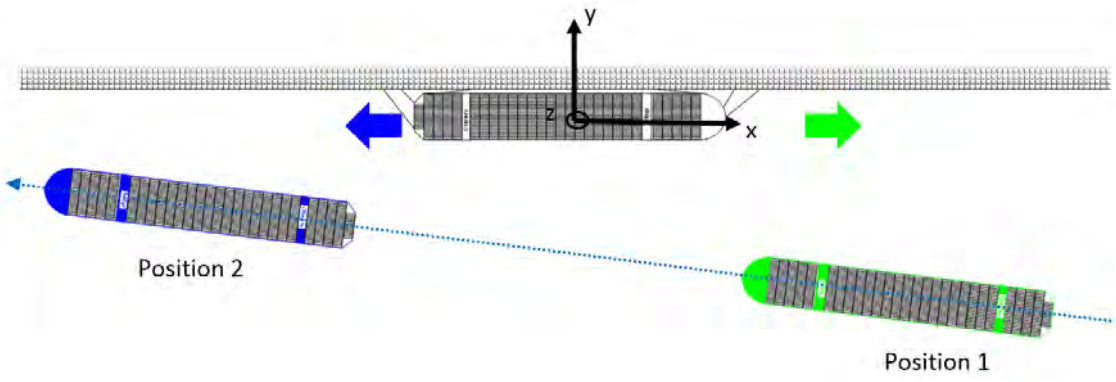

Figure 3-4 : Definition sign convention and axis system O-x,y,z.

4 NUMERICAL MODELS

In order to simulate the behaviour of the moored vessel in the passing event, the effect of several numerical packages needs to be combined, including RoPES (Pinkster Marine Hydrodynamics (PMH)), Octopus Office (ASEA Brown Boveri (ABB) – integration of Seaway, originally developed by J. Journée[4]) and the UGent in-house time domain method Vlugmoor.

4.1 RoPES

The RoPES package has been developed as a joint-industry project (JIP), combing the knowledge of several leading hydrodynamic research institutes. RoPES calculates passing ship forces, using the potential double body flow method (Pinkster, 2014). Figure 3-2 in section 3.3 gives an example of a case generated in RoPES. The theory has its limitations, for example when flow separation zones are present in real life viscous flow. Flow separation typically occurs when ships pass with a non-zero drift angle (van Wijhe and Pinkster, 2008) or in case of entering a narrow channel or lock (Toxopeus and Bhawsinka, 2016). By assuming a rigid water surface, all free surface effects are ignored, including long waves generated by passing vessels (Pinkster, 2004) and their sinkage and trim caused by the water level variations generated by the return flow, known as squat. In order to cope with this last effect, which is a function of the blockage of the wetted section and the passing velocity, the correction factor according to Talstra and Bliek (Talstra and Bliek, 2014), which has been validated using model tests performed at FHR in the framework of RoPES JIP (Delefortrie et al., 2012), is applied on the obtained results from RoPES.

4.2 Octopus office

The reaction of the ship to external forces is largely affected by the hydrodynamic coefficients, which define how much water is moved together with the vessel (added mass) and how the motion damps out. These coefficients are calculated using the 2D strip theory package 'Seaway' (Journée and Adegeest, 2003). As the vessel is moored at a quay with restricted water depth, the coefficients need to be generated for shallow water cases. The Seaway code has been validated for shallow water conditions, using tests performed at the towing tank for manoeuvres in confined waters at FHR, in collaboration with Ghent University (Vantorre and Journée, 2003).

4.3 Vlugmoor

Vlugmoor is the in-house package which calculates the behaviour of moored vessels, based on input from RoPES, Octopus Office and the mooring configuration (see chapter 5). The code solves the force equilibrium in 4 degrees of freedom (surge, sway, yaw and roll), with coupling between sway and yaw. Based on the accelerations of the vessel, the new position of the moored vessel is calculated, using trapezoidal integration. In the current software, mooring line forces are calculated as linear springs. As the behaviour of lines is very often non-linear, certainly for very elastic lines, an overhaul of this module is foreseen for the near future, based on full-scale tests. One of the presented cases below, demonstrates the necessity of including non-linear stress-strain behaviour in the simulation software.

5 MOORING CONFIGURATION

The mooring configuration of the vessel has a large influence on the behaviour of the moored vessel. Even for a given number of lines, the differences between configurations can be significant (see chapter 7). The first component is fixed in the design phase of the vessel, being the number of winches and their position, the position of the fairleads and the characteristics of the lines (maximum breaking load (MBL) and elasticity). The quay equipment, bollards and fenders, cannot be changed easily. There are however operational constraints concerning the mooring configuration as well. The most pronounced one is a spatial configuration of the lines, where the aim should be to come up with a well-balanced mooring plan. The second aspect is the pretension in the lines, which plays a huge role in the ship's behaviour and is especially a challenge in a tidal environment. A lack of pretension in some lines already significantly changes the reaction to the passing vessel, leading to large motions and/or large line forces.

[4] The Knowledge Centre Manoeuvring in Shallow and Confined Water (Flanders Hydraulics Research – Ghent University) wishes to pay tribute to prof. ir. Johan Journée who passed away on December 15th, 2017, at the age of 76.

5.1 Quay equipment

The North Sea Terminal is a dedicated container terminal, with bollards every 21.5 m, combined with high impact fenders at the same positions along the quay wall. Due to the presence of the gantry crane rails, the bollards are positioned close to the vertical quay side. The distance between ship's side and quay, when the ship is held against the fenders due to the pretension in the lines, is equal to the width of the fenders. The distance between the bollards and the ship's hull is taken as 2.0 m.

5.2 Ship equipment

The ship equipment varies highly in between container vessels, which can be explained by the large variety in rope types and sizes. IMO/IACS formulated recommendations in 2005 (IACS, 2005 and IACS, 2014), regarding the MBL of the lines and the number of lines to be used. For newly built container vessels, the more demanding 2016 guidelines (IACS, 2016) has been developed. This new set of guidelines, however, fails at incorporating requirements regarding elasticity of the lines. The mooring lines on board of the vessels C1 and C2 confirm this observation. Table 5-1 gives the number of lines (n_{lines}), the MBL and breaking strain (ε_{br}) of the vessels. Whereas the MBL is similar, the breaking strain varies significantly. For the same external force, vessel C2 will move almost twice as much along the quay compared to vessel C1. Note as well that the lines of vessel C2 are expected to show non-linear stress-strain behaviour.

	C1	C2
n_{lines} [-]	12	12
MBL [ton]	160	143
ε_{br} [%]	15	28

Table 5-1 : Mooring equipment of vessels C1 and C2.

5.3 Lines plan

The mooring lines plan is the end-responsibility of the captain of the vessel, who often receives input from the harbour (in the person of the pilot). At some terminals, there is a fixed mooring plan. This is standard practice at tanker terminals, but not at container terminals. The number of lines however, is imposed by the Antwerp Port Authority. For vessels C1 and C2, a total of 12 lines is demanded (2 fore lines, 2 fore breasts, two fore and two aft springs, 2 aft breasts and 2 aft lines). The exact mooring plan will vary in between vessels and also between two port calls of the same vessel, because of following reasons :

- Conditions (water level, current, wind,…) which were present during the berthing operation.
- Skill of the crew.
- Presence of other vessels at the terminal which limits available bollards at quay.
- Relative position of the vessel with respect to the bollards.

The port of Antwerp delivered some photo material of moored container vessels, as can be seen in Figure 5-1.

Figure 5-1 : Typical mooring configuration of moored 13000 TEU container vessels at North Sea Terminal, using 12 lines. – images courtesy of Antwerp Port Authority

Vessels can be moored portside or starboard side, the latter requiring swinging before berthing. The vessels 'C1' and 'C2' are both moored portside. The lines plan is denoted by the coordinates of the bollards at the quay (x_q, y_q, z_q) and the fairleads of the moored vessel (x_s, y_s, z_s), in the axis system O-x,y,z, which has been defined in Figure 3-4. The top view of the mooring configuration is given in Figure 5-2. The z-coordinates are given with respect to the water surface. They will show slight variations in between the cases, as z_q and z_s depend on the water level and the moored vessel's draft respectively. The levels are given in Table 5-2. Due to the presence of the higher forecastle deck, the fore lines will be steeper than the aft lines, which are located at a lower aft mooring deck. For this validation effort, it is assumed that all lines are pretensioned by default to 10% of the MBL, which is deemed good practice. The fourth passing case shows the importance of the pretension, certainly for highly elastic lines.

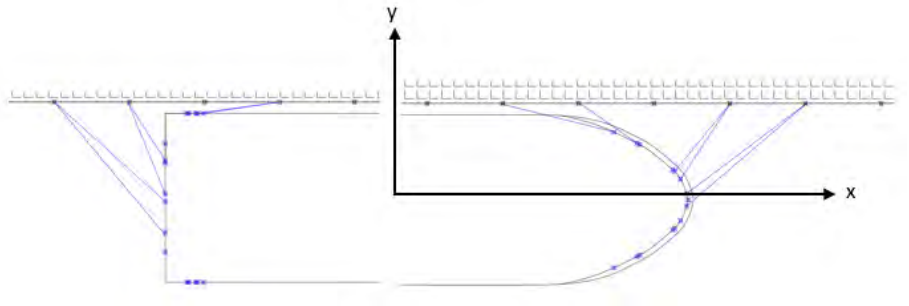

Figure 5-2 : Lines plan C1 and C2, portside mooring.

	z_q [m]	$z_{s,a}$ [m]	$z_{s,f}$ [m]
C1-T	8.77	11.40	17.57
C1-C3	5.28	11.50	17.67
C2-B1	7.24	12.50	18.67
C2-B2	5.40	12.00	18.17

Table 5-2 : Level of the bollards at the quay (z_q), the aft mooring deck ($z_{s,a}$) and the forecastle mooring deck ($z_{s,f}$), relative to the water surface.

6 COMPARING MEASUREMENTS AND SIMULATIONS : VALIDATION

For the four passing events described in section 3, the registered motions, using GPS, are compared with the numerical results from Vlugmoor. The longitudinal motions, following the definitions from Figure 3-4, are plotted as a function of the relative time t_r [s], which is zero at the moment the moored ship starts to move. Using this definition for both numerical and full-scale data, a comparison of both motion amplitude and period can be made.

6.1 Case C1-T

In the first case, a tanker (T) passes the moored container vessel (C1), which has relatively stiff lines on board. Before comparing the results from the Vlugmoor analyses with the measured GPS result, the longitudinal forces calculated by RoPES are examined. The time series is given in Figure 6-1, including the Talstra and Bliek (T&B) correction factor. The negative force (moving the moored vessel astern) is higher than the positive one (pulling the moored vessel ahead), which is due to the inclined trajectory of the passing vessel (Figure 3-1).

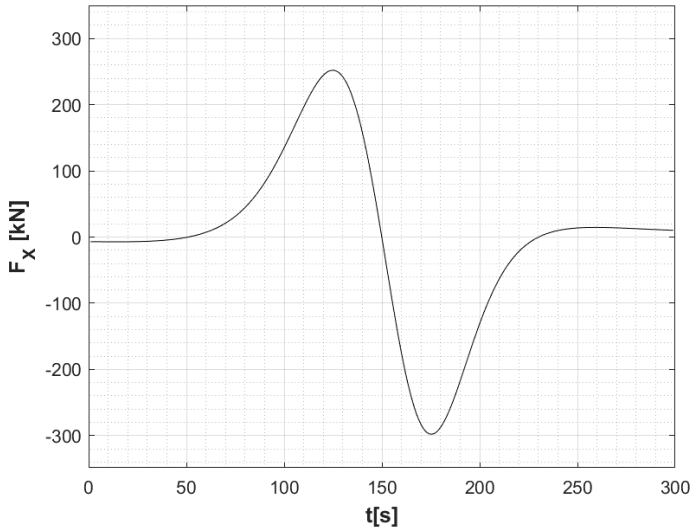

Figure 6-1 : Longitudinal force (F_x) acting on the moored vessel (C1), due to the passing tanker (T). Numerical RoPES results, including T&B correction.

Figure 6-2 compares the measured motion of the moored vessel C1 with the simulation results. It can be observed that the period of the motion is very similar, which means that the calculation of the hydrodynamic masses and the collected AIS data (passing speed and distance) seem correct. The negative motion is significantly larger than the positive motion, which follows from the inclined path of the passing vessel. The motion amplitude is overestimated in the simulation. Both the negative and positive peak are higher than the measured GPS results. This could be allocated to a stiffer reaction of the lines than expected. As the depth-Froude number for this passing event is rather high (Fr_d = 0.42), the correction proposed by Talstra and Bliek is significant. The longitudinal force coming from RoPES needs to be multiplied by the factor 1.25 for all time steps. Figure 6-2 also shows the motions of the moored vessel, according to the uncorrected RoPES output. Additional research, using model tests is needed to validate this RoPES correction factor, as it has a significant influence on the results of the mooring analysis in shallow and confined waters. Awaiting these results, the T&B factor is applied for all cases.

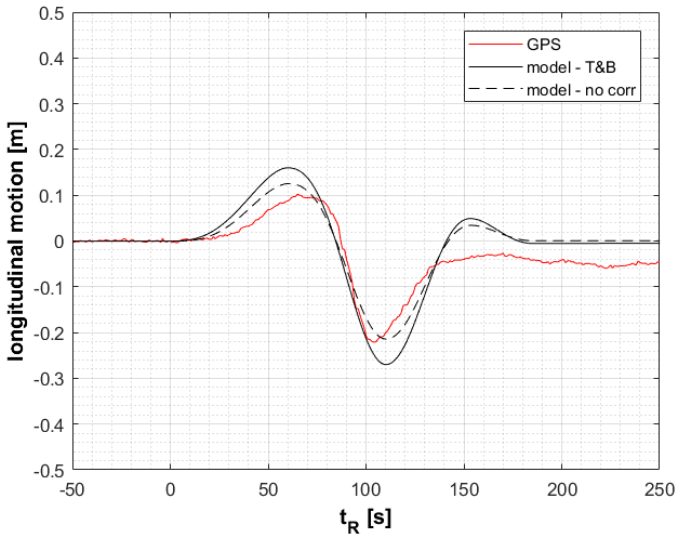

Figure 6-2 : Case C1-T ; Longitudinal motion of the moored vessel : Numerical results with and without T&B correction factor versus GPS measurement.

6.2 Case C1-C3

In this second case, the moored vessel is passed by an Ultra Large Container Vessel, which sails at a lower speed and larger passing distance compared to the tanker. The comparison between GPS

measurements and numerical results is given in Figure 6-3. The total period of the motion is indeed longer, around 250s, with again a good agreement between numerical and measured results. The amplitudes are also very similar in this case. The difference in positive motion might by caused by lower pretension levels in the fore springs and aft lines (see also section 6.4) in reality compared to the simulation assumption (pretension equals 10% MBL).

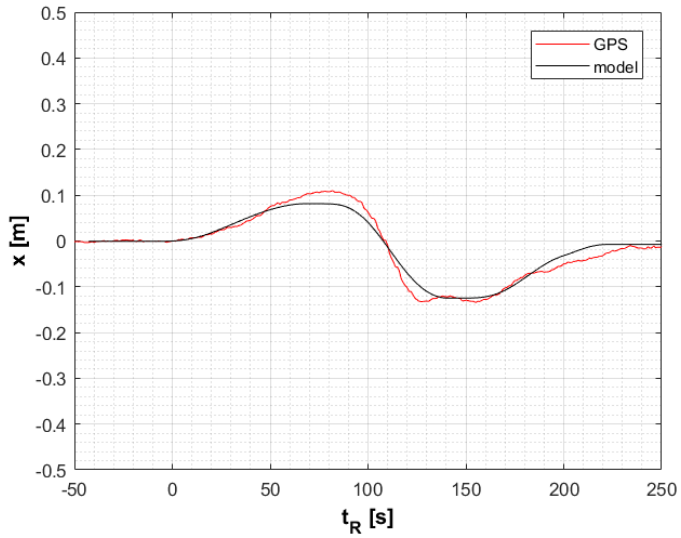

Figure 6-3 : Case C1-C3; Motion of the moored vessel : Comparison GPS and model.

6.3 Case C2-B1

The moored vessel C2 has the same mooring plan, yet the mooring lines have an elongation at break of 28%, compared to the much stiffer lines of the moored C1 vessel. Figure 6-4 shows the comparison between the GPS measurements and the numerical output. The periods of both motions again show good similarity. The GPS measurements, however, show a very large positive motion, which is not expected based on the inclined trajectory of the passing vessel. Here the difference is large with the modelled results, which are more in line with the expectations. The negative amplitude is similar. The difference in positive motion peak might be explained by the non-linear stress-strain behaviour of highly elastic lines. Elastic lines react very elastic at low stress levels, with a gradual stiffness increase with higher line loads. The linearization thus depends on the magnitude of the line forces. If the pretension is low (or absent), the lines show large elongations even at low stress levels. This leads to large ship motions, as displayed in Figure 6-4. The non-linear line behaviour is discussed further in the next section.

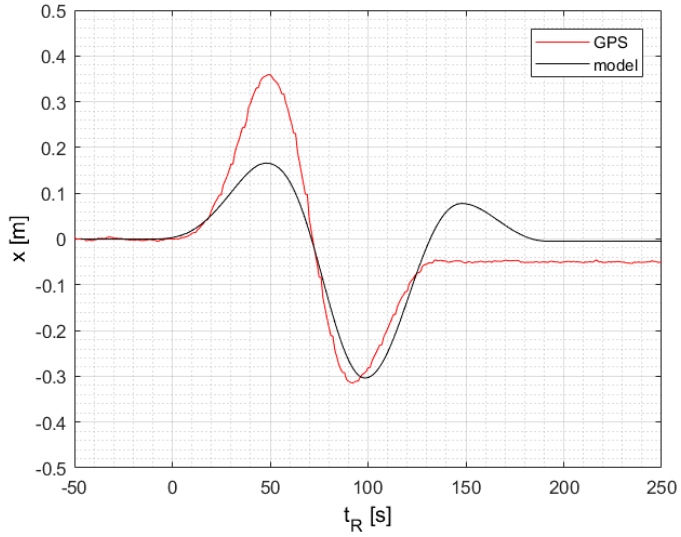

Figure 6-4 : Case C2-B1; Motion of the moored vessel : Comparison GPS and model.

6.4 Case C2-B2

In this last case, the same moored container vessel is passed by a bulk carrier B2, with similar dimensions as the first one (B1). A comparison between the numerical and the measured results is given in Figure 6-5.

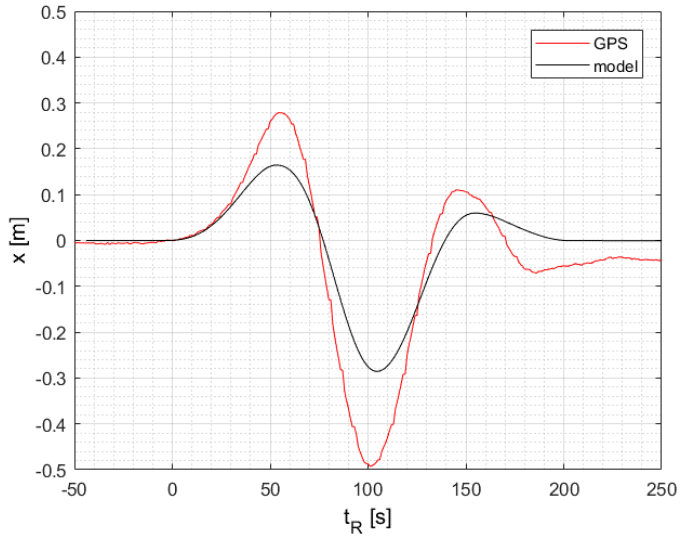

Figure 6-5 : Case C2-B2; Motion of the moored vessel : Comparison GPS and model.

A large discrepancy between GPS measurements and the numerical results is present, when comparing the motion amplitudes. The period of the motion shows decent agreement, which again means that the confidence in the passing vessel's input data and the moored vessel's hydrodynamics is high. The motions, however, are underestimated, in both senses. Again, non-linearity of the lines seems to be the cause of these differences. Without knowing the exact stress-strain curve of the mooring lines, the general curve of a highly elastic material is given in Figure 6-6. Three different linear approximations are shown :

- In case sufficient pretension is present (F_{pr} = 10% MBL), the highly-elastic part of the curve is avoided. If the line loads are high, the green curve is chosen as linear stress-strain factor, which is the average slope of the curve between F_{pr} and MBL.
- In a second case, again pretension level is satisfactory (10% MBL), the forces in the lines during the ship passages remain limited. In this loading zone, the line will react according to the blue line. This approximation is used for case C2-B1 (Figure 6-4) and in Figure 6-5.
- In a third case, the pretension is low (5% F_{br}), which causes the line to react very elastic. The red linearization in Figure 6-6 is used for the simulation shown in Figure 6-7.

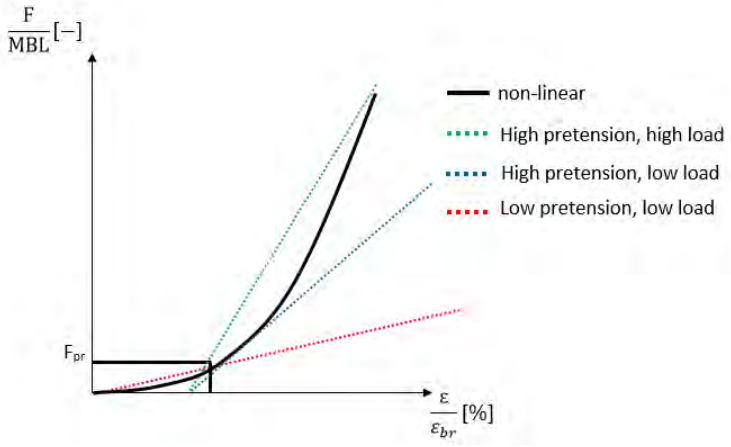

Figure 6-6 : Non-linear stress-strain behaviour highly elastic line : three linear stiffness approximations.

The same passing event is now modelled according to the red stress-strain line in Figure 6-6, which means a 50% stiffness reduction compared to the blue curve. The resulting motions are given in Figure 6-7. The modelled motion amplitude is closer to the measured GPS data. The period becomes larger, due to reduced stiffness of the line, which causes larger motions and consequently a longer period of the motion. Of course, the results shown are again based on a simulation using linear lines, including a lower line stiffness and pretension value. The conclusion here is that a lack of pretension, for non-linearly deforming elastic lines, can lead to high motions, even with relatively low line forces. In order to fully capture this effect, a full non-linear model needs to be implemented in the software.

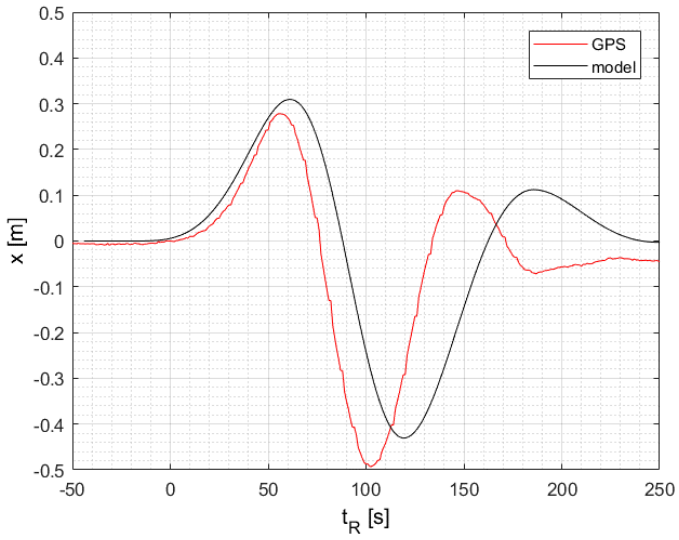

Figure 6-7 : Case C2-B2; Motion of the moored vessel : 5% pretension, reduction of stiffness by 50% compared to the results shown in Figure 6-5.

7 DETAILED STUDY OF THE MOORING PLAN

In this section, the mooring plan of the vessel is examined, from an operational point of view. The starting point of the discussion is the case C1-C3, with the mooring plan given in Figure 5-2 and Table 5-2. The configuration, which consists of 12 lines, is discussed on the level of the individual lines and the configuration as a whole. In a first stage, an efficiency parameter is derived for each line. These are then combined into four parameters, which show the balance and potential of the mooring plan.

7.1 Discussion on the level of the individual lines

The argument is started by looking at the position of the individual lines. The line segment between the bollard on the quay and the fairlead, is given by three coordinates for each point (x,y,z). These six parameters can be expressed as the angles in horizontal and vertical plane (α and β), as well as the length of the line (l), between bollard and fairlead. The total line length (ℓ) is the sum of l and l_{fw}, being the line length between fairlead and winch. By transferring the origin of the axis system to the centre of the bollard, α, β and ℓ are expressed as follows (see Figure 7-1).

$$\beta = \tan^{-1} \frac{z_s - z_q}{\sqrt{(x_s - x_q)^2 + (y_s - y_q)^2}} \tag{1}$$

$$\alpha = \cos^{-1} \frac{x_s - x_q}{\sqrt{(x_s - x_q)^2 + (y_s - y_q)^2}} \tag{2}$$

$$\ell = \sqrt{(x_s - x_q)^2 + (y_s - y_q)^2 + (z_s - z_q)^2} + l_{fw} \tag{3}$$

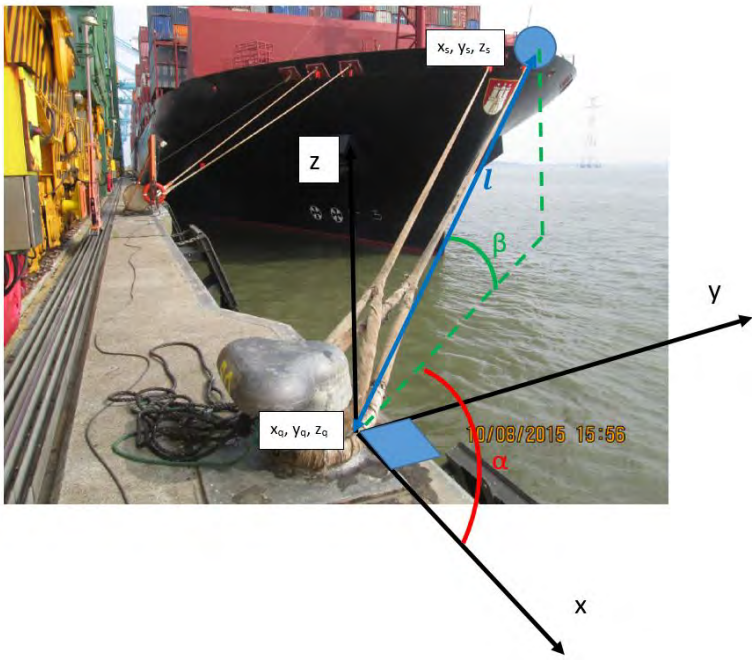

Figure 7-1 : Definition line angles α and β and the length of the line section between bollard and fairlead (*l*).

The values for α, β and ℓ for each line are summarized in Table 7-1.

	α [°]	β [°]	ℓ [m]		α [°]	β [°]	ℓ [m]
Fore lines	140	16	52	**Aft lines**	54	17	32
	144	17	49		65	13	35
	124	27	35		39	8	50
	130	28	32		48	7	61
Fore springs	28	40	43	**Aft springs**	174	17	35
	20	23	48		175	15	37

Table 7-1 : Mooring line angles (α, β) and lengths (ℓ); Mooring configuration C1 (case C1-C3).

Table 7-1 shows that due to the height of the forecastle deck, the fore lines and springs show large angles with the horizontal plane, which means that they will show lower efficiency at taking up horizontal forces, which are of interest here. The fore and aft lines show angles in the horizontal plane (α) between 40° and 60° (140° and 120°), which indicates that they will help at taking up both transversal and longitudinal forces. Breast lines (α close to 90°) are not present in the configuration, indicating that in case of heavy (lateral) wind loads, the capacity of the configuration in the transversal direction might be insufficient. Due to the level and shape of the aft mooring deck, the aft springs are very efficient (α close to 180° and β < 20). The fore springs are hampered by the shape and level of the forecastle, leading to less efficient fore springs. The total of the lines, ℓ, is important when evaluating the efficiency of the lines within the mooring plan. Long lines will react slowly to external forces, whereas short lines will show large strain at smaller deformations, leading to large forces in the lines.

The mooring line angles (α,β) and the line length ℓ are combined in efficiency parameters, expressing the potential for lines to take up longitudinal and transversal loads. In a first step, the lines are presented as force vectors in the 3D space. Based on simple geometrics, the x and y component of the force vector F, which represents the total line force, are given as :

$$F_x = F \cdot \cos\beta \cdot \cos\alpha \;;\; F_y = F \cdot \cos\beta \cdot \sin\alpha \tag{4}$$

In order to build up force, the line needs to elongate. For the longitudinal forces, the potential of the line is expressed as the elongation 'dl', which is present for a longitudinal motion 'dx' (see Figure 7-2). It is assumed that the motion is small compared to the line length. For a line which is located in the x,y-plane, the following is valid, only considering first order terms.

$$l_1^2 - l_0^2 = x_1^2 - x_0^2 \Rightarrow dl \cong \cos\alpha \cdot dx \tag{5}$$

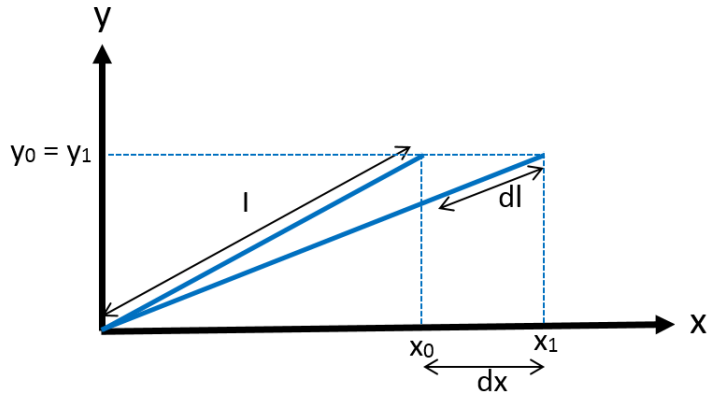

Figure 7-2 : Elongation of the mooring line dl in function of a longitudinal ship motion dx.

Assuming linear behaviour of the line, the force build-up is a linear function of the strain (ε) in the line. Using (eq. 5), this is expressed as :

$$\varepsilon = \frac{dl}{\ell} \cong \cos\alpha \cdot \frac{dx}{\ell} \tag{6}$$

Based on the force components (eq. 4) and the relation between strain and motion components (eq. 6), the efficiency of a line with angles α_i, β_i and length ℓ_i, is given as:

$$e_{Xi} = \cos^2\beta_i \cdot \cos^2\alpha_i \cdot \left(\frac{\ell_i}{\ell_{ref}}\right)^{-1} \tag{7}$$

$$e_{Yi} = \cos^2\beta_i \cdot \sin^2\alpha_i \cdot \left(\frac{\ell_i}{\ell_{ref}}\right)^{-1} \tag{8}$$

$$\ell_{ref} = \frac{1}{n} \cdot \sum_{i=1}^{n} \ell_i \tag{9}$$

In (eq. 7) and (eq. 8), ℓ_{ref}, the average line length, is added to non-dimensionalise the efficiency parameters. The resulting efficiency parameters for all lines are given in Table 7-2.

	e_{Xi} [-]	e_{Yi} [-]		e_{Xi} [-]	e_{Yi} [-]
Fore lines	0.45	0.31	**Aft lines**	0.41	0.78
	0.52	0.27		0.20	0.96
	0.30	0.67		0.50	0.34
	0.43	0.60		0.31	0.37
Fore springs	0.45	0.12	**Aft springs**	1.09	0.01
	0.68	0.09		1.06	0.01

Table 7-2 : Efficiency of the lines in mooring configuration C1 (case C1-C3).

The conclusions are similar to the ones made based on the angles α and β (Table 7-1), but the results can be interpreted more easily, as the angles are rewritten as two efficiency parameters, for both longitudinal and transversal directions. The parameters also include the effect of the line length on the reaction of the line to external loads. For the longitudinal direction, the most efficient lines are the aft springs (e_{Xi} = 1.09 and 1.06), combining favourable line angles and relatively short lines, which leads to an efficiency larger than the unity. The fore springs only show efficiencies of 0.45 and 0.68, due to the large vertical angle and inclination with respect to the quay wall in the horizontal plane. Due to the absence of breast lines, the lateral efficiency of all lines is limited. Only two of the aft lines reach values of 0.78 and 0.96. As can be expected, the fore and aft springs have a negligible contribution towards taking up lateral forces, with e_{Yi} values between 0.01 and 0.12.

7.2 Discussion on the level of the mooring plan

The definition of the efficiencies of the singular lines allows to evaluate and compare mooring plans, both for the same vessel and in between different vessels. Focussing on the quality of the mooring plan of a given vessel (design parameters fixed), e_{Xi} and e_{Yi} are translated in the following efficiency parameters.

$$e_{Xp} = \sum_{i=1}^{n_{\alpha<90}} \cos^2 \beta_i \cdot \cos^2 \alpha_i \cdot \left(\frac{\ell_i}{\ell_{ref}}\right)^{-1} \quad (10)$$

$$e_{Xn} = \sum_{i=1}^{n_{\alpha>90}} \cos^2 \beta_i \cdot \cos^2 \alpha_i \cdot \left(\frac{\ell_i}{\ell_{ref}}\right)^{-1} \quad (11)$$

$$e_{Yf} = \sum_{i=1}^{n_f} \cos^2 \beta_i \cdot \sin^2 \alpha_i \cdot \left(\frac{\ell_i}{\ell_{ref}}\right)^{-1} \quad (12)$$

$$e_{Ya} = \sum_{i=1}^{n_a} \cos^2 \beta_i \cdot \sin^2 \alpha_i \cdot \left(\frac{\ell_i}{\ell_{ref}}\right)^{-1} \quad (13)$$

e_{Xp} and e_{Xn} express the capability of the configuration to deal with positive and negative longitudinal forces. For the transversal direction, e_{Yf} and e_{Ya} are defined, which show the potential to take up lateral forces on the fore and aft of the vessel. For the mooring plan for the C1-C3 case, given in Figure 5-2, these four parameters are given in Table 7-3.

e_{Xp} [-]	e_{Xn} [-]	e_{Yf} [-]	e_{Ya} [-]
2.55	3.85	2.07	2.47

Table 7-3 : Efficiency of the mooring plan C1 (case C1-C3, Figure 5-1).

The mooring plan efficiencies as given in (eq. 10) to (eq. 13) and Table 7-3 are only suited to evaluate different mooring plans for the same vessel. In order to make a comparison in between different vessels possible, several additional terms need to be added to the equation, including amongst others:

- The (total) number of lines.
- The breaking strength and elasticity of the lines, relative to a reference value, should be included in a similar way as the line lengths are represented. In case of mooring lines showing non-linear stress-strain curves, this process becomes more complex.
- Linked to the previous bullet, a correction factor for pretension of the lines.

Future research will include further development of the efficiency parameters by comparing different vessels' mooring configurations and simulation results. The next section focusses on the application of the efficiency parameters to evaluate mooring plans for the C1 vessel.

7.3 Study of the mooring plan for case C1-C3

The starting point for this section is the mooring plan which has been used for the validation study, given in Figure 5-2 and repeated below in Figure 7-3, indicated as plan I. The second plan aims at optimising the configuration to cope with longitudinal forces, which is the case for passing ship events. Note that at busy terminals, limited distance in between moored vessels often makes it impossible to achieve this configuration. The fore spring position is also adjusted, to increase its efficiency, as the efficiency parameter e_{Xi} for this line is low (0.45,Table 7-2). By adjusting its position, this efficiency increases from 0.45 to 0.59. The fore and aft lines are positioned to limit the angles α and β. The downside of this repositioning is the increase in line lengths, which leads to less reactive lines. This is taken into account by keeping the reference length, ℓ_{ref}, constant for the three cases, as the average length of all lines in plan I. Plan III is very compact, which occurs when multiple vessels, in some cases larger than the design vessel, are moored at the quay, minimising the available bollard space for the fore and aft lines.

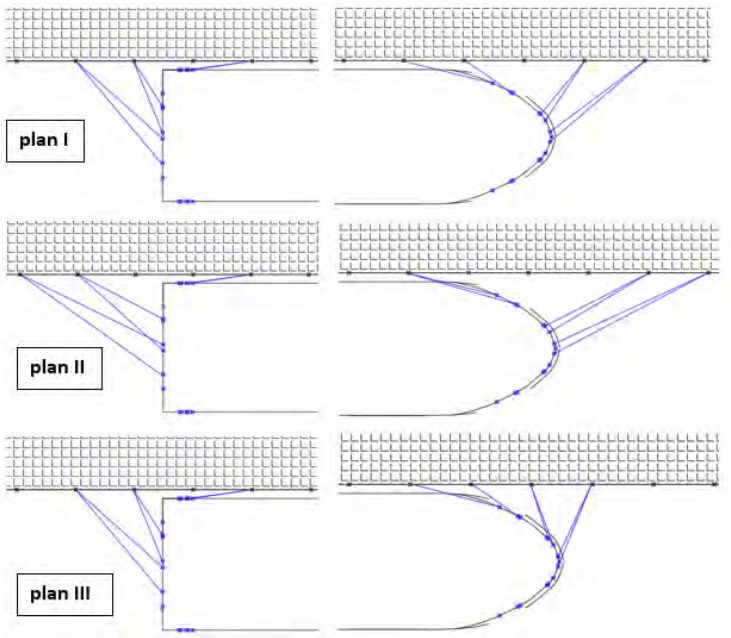

Figure 7-3 : Case study C1-C3 : mooring plan I (validation study, Figure 5-1), plan II and plan III.

The efficiency parameters for the configurations given in Figure 7-3 are given in Table 7-4.

Plan	e_{Xp}	e_{Xn}	e_{Yf}	e_{Ya}
I	2.55	3.85	2.07	2.47
II	3.37	4.36	0.69	0.79
III	2.77	2.48	3.61	2.47

Table 7-4 : Efficiency of the mooring plans I,II and III, case C1-C3.

Table 7-4 parameterizes the above description of the mooring plans. In the second plan, the longitudinal efficiency increases, whereas the transversal capacity is lowered significantly. In the passing events at hand however, the transversal forces are small, which limit the impact of said decrease in lateral efficiency. In the third plan, the efficiency in the negative longitudinal sense (e_{Xn}) decreases, the lateral efficiency of the fore lines (e_{Yf}) on the other hand, is augmented. This configuration is thus not balanced in the lateral direction and will show yaw rotation under large lateral forces. Figure 7-4 compares the longitudinal motions for the three plans, where it can be clearly observed that the efficiency parameters indeed give a good indication for the impact of the change in mooring plan on the longitudinal motions.

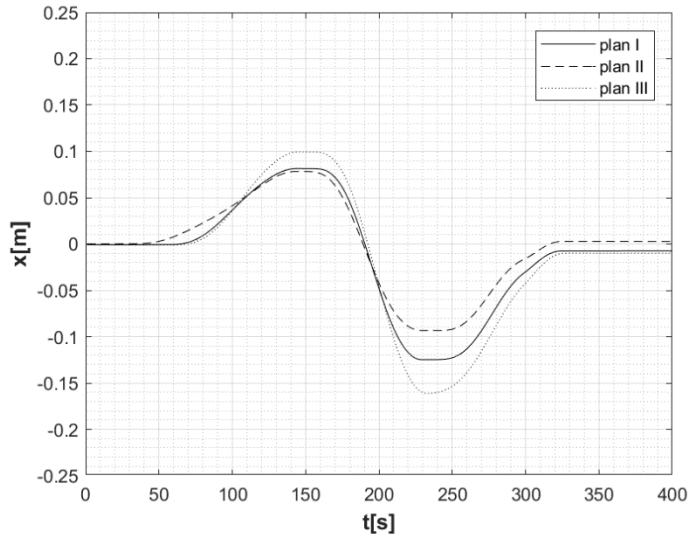

Figure 7-4 : Modelled longitudinal motion C1-C3, mooring plan I,II and III.

8 CONCLUSION

This paper elaborates on the validation of the UGent in-house software package Vlugmoor, which models the behaviour of moored vessels, using motion measurements performed at North Sea Terminal in the Port of Antwerp. Four events are considered, with four different passing vessels, the moored vessel being a 13 000 TEU container vessel in each case. In the first two cases, the moored vessel has relatively stiff mooring lines, which react in a linear way. The period of the motion as well as the motion amplitude show good agreement in between the GPS measurements and numerical results. The largest deviation is observed with the passage of the tanker, where the passing speed is reasonably high. This leads to a large correction factor, according to Talstra and Bliek, for the longitudinal forces due to the passing vessel. This factor should be the subject of future validation work, focussing on passing events in sections with rather high blockages and Froude numbers.

In the next two cases, the moored vessel has elastic mooring lines, which are known for showing a highly non-linear stress-strain behaviour. In the first of these two events, a linear approximation of the elasticity seems to predict the motion peak well, but not the entire motion time series. In the second one, the linear formulation falls short to predict the motion peaks, as well as the full time dependent behaviour. This is because in cases with small pretension force and moderate line forces, the stiffness of the lines in this region of the stress-strain curve is limited. Reducing the modelled stiffness by 50% leads to better agreement with the measured motions, however the motion period differs more from the measurements. There must be concluded that in case of highly elastic lines and low pretension force, the current linear model for the elasticity is insufficient to predict the motions accurately. An overhaul of the model is planned, based on the results of full-scale experiments on lines. In general, use of highly elastic lines leads to large motions, certainly when the pretension level is not kept at an adequate level (generally around 10% MBL), during the stay at the berth. In the presence of tidal current and associated water level change, accompanied by draft variation during loading, this requires a continuous effort of the ship's crew.

The paper discusses a first effort to come up with efficiency parameters, which define the potential of a line to take up longitudinal and transversal forces in the horizontal plane. Based on force and strain considerations, the efficiency parameters e_X and e_Y are defined as a function of the line angles and the line length. These efficiency parameters are used to identify the most (in) efficient lines, in function of the orientation of the external load, and to perform targeted adjustments to the position of the lines. In reality the practical constraints of the operational container terminal, including the distance between moored vessels, has to be taken into account. The balance and performance of the mooring configuration is summarized using four efficiency parameters, denoting the suitability to take up longitudinal and lateral forces. A simple example is given, where starting from the mooring plan used for validation, a change of the lines' position, influences the performance of the configuration significantly. Further work into the potential of these coefficients is scheduled.

Acknowledgement

The authors would like to thank Cynthia Pauwels of the Antwerp Port Authority, for her help in providing support regarding the GPS measurements and logged passing parameters at the North Sea Terminal.

REFERENCES

Delefortrie, G., Vantorre, M., Capelle, J., Ides, S., (2012) “The Effect of Shipping Traffic on Moored Ships.”, in: 10th International Conference on Hydrodynamics October 1-4, St. Petersburg, Russia. pp. 1–6.

IACS, (2016) “Anchoring, Mooring, and Towing equipment.”

IACS, (2014) “IACS : Requirements concerning mooring, anchoring and towing.”

IACS, (2005) ”IACS : Rec. No. 010 : Equipment.”

Ides, S., Pauwels, C., Torfs, P., (2018) “Motions of moored vessels due to passing vessels : full-scale measurements at a container terminal in the Port of Antwerp.”, in: PIANC World Congress Panama.

Journée, J.M., Adegeest, L.M.J., (2003) “Theoretical Manual of Strip Theory Program “SEAWAY for Windows”.”, Report 1370.

PIANC, (2012) “Report n° 115 - Criteria for the (Un)loading of Container Vessels”.

Pinkster, J.A., (2004) “The influence of a free surface on passing ship effects.”, Int. Shipbuild. Prog. 61, pp. 313–338.

Pinkster, J.A., Pinkster, H.J.M., (2014) “A fast, user-friendly, 3-D potential flow program for the prediction of passing vessel forces.”, in: PIANC World Congress. San Francisco, USA.

Port of Antwerp, (2017) “2017 Facts and Figures.”

Port Today, (2018) “https://port.today/msc-cma-cgm-open-door-megamax-24-era/” , accessed 15/03/2018.

Talstra, H., Bliek, A.J., (2014) “Loads on moored ships due to passing ships in a straight harbour channel.”, in: PIANC World Congress. San Francisco, USA, pp. 19.

Toxopeus, S.L., Bhawsinka, K., (2016) “Calculation of hydrodynamic interaction forces on a ship entering a lock using CFD.”, in: Proceedings of 4th MASHCON (BAW), Karlsruhe, Germany, Hamburg, Germany, pp. 305–314.

van Wijhe, H.J., Pinkster, J.A., (2008) “The effects of ships passing moored container vessels in the Yangtzehaven, Port of Rotterdam.”, in: International Conference on Safety and Operations in Canals and Waterways. Glasgow, UK, pp. 117–130.

Van Zwijnsvoorde, T., Vantorre, M., (2017) “Safe Mooring of Large Container Ships at Quay Walls Subject to Passing Ship Effects.”, Int. J. Marit. Eng. 159(A4), pp. 467–476.

Vantorre, M., Journée, J.M.J., (2003) “Validatie van het scheepsbewegingenprogramma SEAWAY met behulp van zeegangsproeven in ondiep water.”, in: Numerical Modelling Colloquium, Flanders Hydraulics Research, Antwerp, October 2003. pp. 1–22. (Dutch)